

# Modulation of Ligand Selectivity Associated with Activation of the Transmembrane Region of the Human Follitropin Receptor

LUCIA MONTANELLI, JOOST J. J. VAN DURME, GUILLAUME SMITS, MARCO BONOMI, PATRICE RODIEN, ERIC J. DEVOR, KRISTIN MOFFAT-WILSON, LEONARDO PARDO, GILBERT VASSART, AND SABINE COSTAGLIOLA

*Institut de Recherche Interdisciplinaire en Biologie Humaine et Moléculaire, Université Libre de Bruxelles (L.M., J.J.J.V.D., G.S., M.B., G.V., S.C.), Campus Erasme, B-1070 Brussels, Belgium; Service de Génétique Médicale (G.S., G.V.), Hôpital Erasme, B-1070 Brussels, Belgium; Department of Endocrinology (L.M.), University of Pisa, 54126 Pisa, Italy; Institute of Endocrine Sciences (M.B.), University of Milan, Istituto Auxologico Italiano Istituto di Ricovero e Cura a Carattere Scientifico, Milan 20145, Italy; Institut National de la Santé et de la Recherche Médicale Equipe Mixte U0018 (P.R.), Angers 49035, France; Molecular Genetics and Bioinformatics (E.J.D., K.M.-W.), Integrated DNA Technologies, Coralville, Iowa 52241; and Laboratori de Medicina Computacional (L.P.), Unitat de Bioestadística and Institut de Neurociències, Universitat Autònoma de Barcelona, 08193 Bellaterra, Spain*

Recently, three naturally occurring mutations in the serpentine region of the FSH receptor (FSHr) (D567N and T449I/A) have been identified in three families with spontaneous ovarian hyperstimulation syndrome (OHSS). All mutant receptors displayed abnormally high sensitivity to human chorionic gonadotropin and, in addition, D567N and T449A displayed concomitant increase in sensitivity to TSH and detectable constitutive activity. In the present study, we have used a combination of site-directed mutagenesis experiments and molecular modeling to explore the mechanisms responsible for the phenotype of the three OHSS FSHr mutants. Our results suggest that all mutations lead to weakening of interhelical locks between transmembrane helix (TM)-VI and TM-III, or

TM-VI and TM-VII, which contributes to maintaining the receptor in the inactive state. They also indicate that broadening of the functional specificity of the mutant FSHr constructs is correlated to their increase in constitutive activity. This relation between basal activity and functional specificity is a characteristic of the FSHr, which is not shared by the other glycoprotein hormone receptors. It leads to the interesting suggestion that different pathways have been followed during primate evolution to avoid promiscuous stimulation of the TSHr and FSHr by human chorionic gonadotropin. In the hFSHr, specificity would be exerted both by the ectodomain and the serpentine portion. (*Molecular Endocrinology* 18: 2061–2073, 2004)

THE LH/CG (CHORIONIC GONADOTROPIN) receptor (LH/CGr), TSH receptor (TSHr), and FSH receptor (FSHr) are encoded by paralogous genes belonging to the large family of rhodopsin-like G protein-coupled receptors (GPCRs) (1–4). They constitute the subfamily of glycoprotein hormone receptors (GpHRs), themselves members of the wider leucine-rich repeats (LRRs) containing GPCR (LGR) family (5) presenting large amino terminal extensions containing

Abbreviations: AFU, Arbitrary fluorescence units; CG, chorionic gonadotropin; FACS, fluorescence-activated cell sorting; FSHr, FSH receptor; GPCR, G protein-coupled receptor; GpHR, glycoprotein hormone receptor; h, human; LGR, LRR containing GPCR; LH/CGr, LH/CG receptor; LRR, leucine-rich repeat; OHSS, ovarian hyperstimulation syndrome; rh, recombinant human; rmsd, root mean square deviation; TM, transmembrane helix, TSHr, TSH receptor; wt, wild-type.

***Molecular Endocrinology* is published monthly by The Endocrine Society (<http://www.endo-society.org>), the foremost professional society serving the endocrine community.**

LRRs. Numerous studies with GpHR chimeras, and site-directed mutagenesis experiments, have demonstrated a clear-cut dichotomy between the structures involved in recognition and binding of their agonists, and generation of the activation signal. Binding and specificity of hormone recognition is encoded in residues belonging to the  $\beta$ -strands of the LRRs (6–11). These are thought to constitute the concave surface of a horseshoe-like structure typical of all LRR-containing proteins (12). The rhodopsin-like, serpentine domain of GpHRs contains seven transmembrane helices (TM) with many but not all the molecular signatures of rhodopsin. As such, the serpentine domain of GpHRs has been shown to relay the signal resulting from hormone binding to the interior of the cell, where it promotes mainly cAMP accumulation via activation of Gs (3).

The intramolecular mechanisms involved in transduction of the activation signal, from the binding step to the activation of the G protein, are the subject of

intense investigation (10, 13–16). Whereas in most rhodopsin-like GPCRs, there is evidence for a direct activating interaction between agonists and the serpentine domains (17–19), recent models for activation of GpHRs suggest that binding of the hormones to the receptors would promote a conformational change in their ectodomains, transforming them into full agonists of the serpentine domain (14). These models are mainly based on experiments with constitutively active, or truncated mutant receptors.

A wide spectrum of spontaneous gain of function mutations has been identified, mainly in the serpentine domains of the TSHr and the LH/CGr (20, 21). They are responsible for target tissue autonomy, resulting in hereditary (22) or congenital (23) toxic thyroid hyperplasia (24) and toxic thyroid adenoma (20), or pseudoprecocious puberty of the male (25), respectively. Investigation of the impact of some of these mutations on structural models of GpHRs elaborated on the template of rhodopsin crystal (26) are yielding information on the mechanism of activation of GPCRs (1, 13, 27). The FSHr has been shown to be more refractory to activation by mutations (28, 29), with only one case reported, characterized by persistent fertility in a male despite pituitary insufficiency (30).

Preservation of tight recognition specificity barriers during coevolution of GpHRs and the  $\beta$ -subunits of the glycoprotein hormones poses an interesting problem in higher primates. In other mammals, circulating hormone concentrations match receptor sensitivity (in the low nanomolar range) for each pituitary hormone-receptor couple. In contrast, during human (h) pregnancy, hCG, which uses the same receptor as LH, reaches circulating concentrations, which are several orders of magnitudes higher (31). There is presently no satisfactory hypothesis for the physiological role of such disproportionately high levels of hCG. However, among the consequences is the possibility of spillover phenomena involving the TSHr (31) or FSHr.

One familial case of pregnancy thyrotoxicosis has been described with a mutation rendering the TSHr abnormally sensitive to hCG (32). As expected, the mutation affected a residue in the LRR portion of the ectodomain of the receptor, which allowed to interpret the phenotype in the lights of the available structural and activation models (33). More recently, mutants of the FSHr have been identified in three families with spontaneous ovarian hyperstimulation syndrome (OHSS) (34–36). The mutant receptors displayed abnormally high sensitivity to hCG, thus providing a satisfactory pathophysiological explanation to the phenotype. However, in all cases, the mutations affected residues of the serpentine portion of the receptor, which challenges our current structural and functional models. In addition, two of the mutant receptors (D6.30<sup>567</sup>N and T3.32<sup>449</sup>A; see *Materials and Methods* for numbering system) were reported to display concomitant increase in sensitivity to TSH, together with detectable constitutive activity (34, 36).

In the present study, we have used a combination of site-directed mutagenesis experiments and molecular

modeling to explore the mechanisms responsible for the phenotype of the three OHSS FSHr mutants. Our results suggest that all mutations lead to weakening of interhelical locks between TM-VI and TM-III, or TM-VI and TM-VII, which contribute to maintaining the receptor in the inactive state. They indicate that broadening of the functional specificity of the mutant hFSHr is correlated to their increase in constitutive activity.

## RESULTS

Before we can attempt to establish a relation between constitutive activity of 3.32 and 6.30 FSHr mutants and their promiscuous stimulation by hCG or TSH, it was necessary to demonstrate that we can reliably compare constitutive activity of the various mutants, despite wide differences of expression at the cell surface. cAMP production in COS cells transfected with various amounts of four mutant constructs was plotted as a function of surface expression, measured by flow immunocytometry (Fig. 1). No deviation from linearity was observed for any mutant. This demonstrates the validity of a normalization method in which cAMP results are divided by flow immunocytometry results (normalized constitutive activity; see *Materials and Methods*). The results in Fig. 1 illustrate also the very low, if any, constitutive activity of the wild-type (wt) FSHr.

### D6.30<sup>567</sup> Mutants

When analyzed functionally by transient expression in COS-7 cells, substitution of aspartate in position 567 of the FSHr into asparagine (D6.30<sup>567</sup>N) is responsible for increase in basal activity of the mutant, together with partial lowering of its specificity toward both hCG

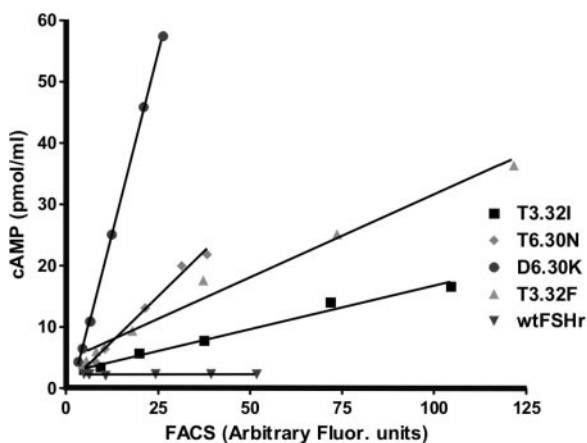


**Fig. 1.** Linearity between Surface Expression of FSHr Constructs and cAMP Production

Linear relation between receptor expression, as measured by flow immunocytometry, and intracellular levels of cAMP achieved in COS cells transfected with increasing amounts of receptor DNA.

and TSH (34). To explore whether the observed phenotype resulted from rupture of chemical bonds or creation of novel bonds, a series of mutants were engineered in which D6.30<sup>567</sup> was replaced by 11 different amino acids (N, Y, H, V, G, A, K, R, T, W, Q) with diverse physicochemical properties. After transient expression in COS-7 cells, expression at the cell surface was measured with the monoclonal antibody 5B2 (34) and basal intracellular cAMP accumulation was assayed (Table 1). As already noted, wide differences were observed in the level of expression of individual mutants, ranging from 11.84 AFU (arbitrary fluorescence units) to 44.08 AFU (Table 1). Only the D6.30W mutant did not reach the cell surface at all. Mutant D6.30Q was similar to the wt FSHr in that it showed virtually no constitutive activity (Table 1). In contrast, all others mutants displayed readily measurable basal activity. Calculation of the ratio between cAMP measurements and fluorescence-activated cell sorting (FACS) results (see *Materials and Methods*) allowed comparison of the constitutive activity of the various mutants (Table 1). D6.30K, D6.30R, and D6.30Y showed the highest cAMP/FACS ratio. The increase in basal activity of D6.30N and D6.30G mutants confirmed the findings by Smits *et al.* (34) and Gromoll *et al.* (30), respectively, in a patient with spontaneous OHSS and a male with preserved fertility despite pituitary insufficiency.

All FSHr mutants were tested for their ability to be stimulated by recombinant human (rh) FSH, rhTSH, and rhCG (Fig. 2, A and B). As expected, all of them responded readily to rhFSH, as did the wt FSHr (Fig. 2A). In addition, all mutants, except D6.30Q, displayed an increase in sensitivity to stimulation by rhTSH, when compared with the wt FSHr, with D6.30N, D6.30G, and D6.30R showing the greatest response

(Fig. 2A). Similarly, most mutants could be stimulated by various concentrations of rhCG (30 IU/ml, 100 IU/ml, 300 IU/ml). D6.30N, D6.30H, D6.30G, and D6.30K

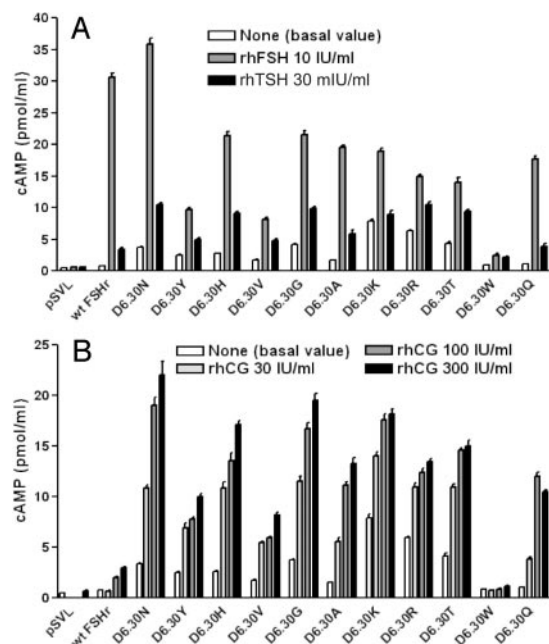


**Fig. 2.** Functional Characterization of D6.30 FSHr Mutants. A, Levels of cAMP observed with cells transfected with empty pSVL vector, wt hFSHr, and D6.30<sup>567</sup> mutants after stimulation with rhFSH (10 IU/ml) and rhTSH (30 mIU/ml) and (B) after stimulation with increasing concentrations of rhCG. COS-7 cells transiently transfected with the various constructs were stimulated by the hormones and intracellular cAMP was determined by RIA. Each graph represents the results of at least two separate experiments. *I* bars represent SE.

**Table 1.** Structure-Function Characteristics of D6.30 Mutants

Construct	Bond Type	H-Bonds <sup>a</sup>	FACS (AFU) (Raw Values) <sup>b</sup>		Basal cAMP (pmol/ml) (Raw Values) <sup>b</sup>		cAMP/FACS <sup>c</sup>	Promiscuous Activation
			Mean	Range	Mean	SEM		
pSVL			9.6	±0.53	1.20	0.07		
wt = D6.30	Salt bridge	1	44.08	±2.91	1.67	0.03	1.36	No
D6.30N	Polar	1	33.04	±1.17	9.09	0.24	33.68	rhCG + rhTSH
D6.30Q	Polar	2	36.63	±1.89	2.61	0.09	5.22	rhCG
D6.30H	Polar	1	29.36	±0.90	7.50	0.13	31.93	rhCG + rhTSH
D6.30A			32.89	±0.30	3.97	0.08	11.92	rhCG + rhTSH
D6.30T			22.32	±0.18	9.56	0.26	65.83	rhCG + rhTSH
D6.30Y			11.84	±0.01	6.61	0.20	244.25	rhCG + rhTSH
D6.30V			12.13	±0.52	3.85	0.20	105.73	rhCG + rhTSH
D6.30G			24.56	±0.24	9.05	0.48	52.58	rhCG + rhTSH
D6.30K			24.23	±0.48	16.91	0.54	107.55	rhCG + rhTSH
D6.30R			17.87	±0.03	13.65	0.77	150.88	rhCG + rhTSH
D6.30W			9.56	±0.76	1.87	0.21		

<sup>a</sup> Number of hydrogen bonds observed in the molecular dynamics simulations.

<sup>b</sup> Results from one representative experiment out of a total of two or three experiments.

<sup>c</sup> Basal cAMP was normalized to cell surface expression for each construct, and values were multiplied by 100 for clarity (see *Materials and Methods*).

were particularly sensitive (Fig. 2B). These results confirm and extend previous observations made with the D6.30N mutant by Smits *et al.* (34).

### Molecular Modeling of the 3.50–6.30 Ionic Lock

In an attempt to provide a structural basis to the observed phenotype of the D6.30 mutants, we performed molecular dynamics simulations for the wt receptor and five mutants, using bovine rhodopsin (26) as template (summarized in Table 1 and Fig. 3). An ionic interaction between D6.30 and R3.50 is believed to contribute to a structural lock between the cytoplasmic ends of TM-III and TM-VI characteristic of the inactive conformation of many rhodopsin like GPCRs (1, 3, 37–39) (Fig. 3A). In this model, a single N-H group of R3.50 is interacting with the O $\delta$ -atom of D6.30 (Fig. 3A).

The D6.30N (Fig. 3B) or D6.30Q (Fig. 3C) mutants replace the ionic pair between TM-III and VI (R3.50–D6.30) by a charged hydrogen bond (R3.50–N6.30 or R3.50–Q6.30, respectively). However, the shorter side chain of N6.30 forms a single hydrogen bond with R3.50, whereas the larger side chain of Q6.30 is able to form two hydrogen bonds. This might explain the different behavior in terms of constitutive activity of

both mutants. Although Q6.30 can maintain the TM-III–VI interaction through two hydrogen bonds, the single hydrogen bond of N6.30 decreases the interaction between both helices leading to constitutive activity (see Table 1). Of note, the D6.30Q mutant responded promiscuously to stimulation by hCG.

Similarly, replacing D6.30 with H (Fig. 3D) makes the interaction with R3.50 similar to N6.30 in the D6.30N mutant: a single hydrogen bond is formed between both helices (Fig. 3D). In concordance, the D6.30H mutant exhibits constitutive activity (Table 1).

The D6.30T mutant (Fig. 3E) needs special attention. The Thr side chain can basically adopt the *gauche*<sup>+</sup> or *gauche*<sup>−</sup> rotamer conformation when located in  $\alpha$ -helices. In the most stable *gauche*<sup>+</sup> rotamer the methyl group of T6.30 points toward R3.50, preventing any interaction between R3.50 and TM-VI (Fig. 3E). The same reasoning can be applied to the poorly expressed D6.30V mutant, which also introduces a  $\beta$ -branched side chain. The intolerance to large bulky residues at position 6.30 is further demonstrated by the D6.30Y and D6.30W constructs. Whereas the D6.30Y exhibits fairly low expression, the D6.30W mutant does not reach the cell surface, probably due to severe misfolding of the protein.

Conversely, because alanine cannot make polar side chain interactions, one would expect the D6.30A mutant to display a larger increase in basal activity than the N or H mutants. However, this is not observed, because D6.30A shows lower constitutive activity. An explanation may be found in the ability of R3.50 to form hydrogen bonds with the backbone carbonyl of A6.30 (Fig. 3F), hereby establishing a stabilizing interaction between TM-III and TM-VI. This is indeed feasible because, unlike threonine or valine, alanine is not  $\beta$ -branched and leaves space between the two helices for such an interaction.

Finally, replacing the D6.30 side chain with a basic Lys or Arg residue enforces a repulsion between the latter and R3.50 (not modeled), leading to a high degree of constitutive activity (Table 1).

In summary, our simulations show that the level of constitutive activity of the mutant receptors is related to the nature of the interaction that can be established between positions 6.30 and R3.50. wt Basal activity (*i.e.* a silent receptor) is either achieved by an ionic interaction or by at least two hydrogen bonds connecting positions 6.30 and R3.50 (see D6.30Q in Table 1 and Fig. 3C). Any residue at position 6.30 resulting in weakening of the 6.30–R3.50 interactions between the cytoplasmic ends of TM-III and TM-VI renders the hFSHr constitutively active, and an ionic lock is needed to avoid promiscuous stimulation by hCG.

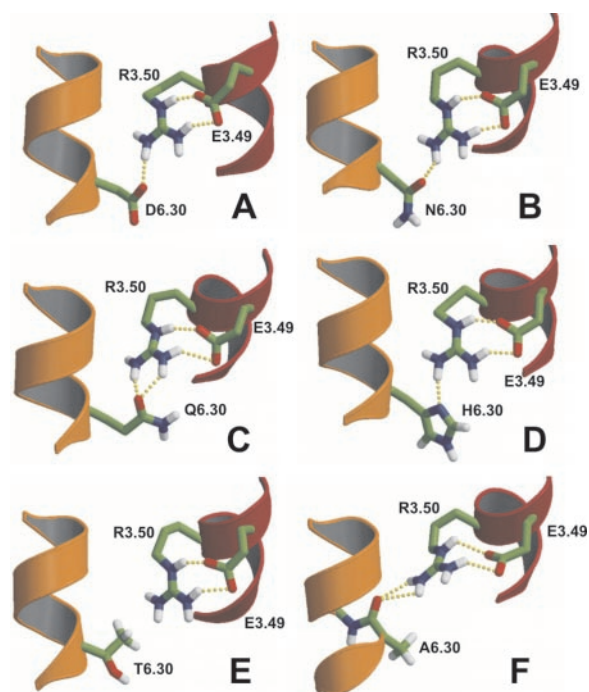


**Fig. 3.** Representative Structures of the Different Models for the 6.30 Mutant Series

For each of the models, a representative structure was selected from the set collected during the molecular dynamics simulations. A, D6.30 wt; B, D6.30N; C, D6.30Q; D, D6.30H; E, D6.30T; and F, D6.30A. Helices are represented as *ribbons*, where side chains involved in the investigated interactions are represented as *sticks*. Backbones of transmembrane helices III and VI are colored in *red* and *orange*, respectively.

### T3.32<sup>449</sup> Mutants

Considering that, similar to D6.30N, mutation of threonine in position 3.32 of the FSHr into isoleucine has been shown to cause increase in sensitivity to hCG (35, 36), we decided to explore the phenotype of a

series of 3.32 mutants in which threonine 449 was replaced by nine different amino acids (I, R, D, F, Y, G, A, N, S). All constructs were well expressed at the cell surface of transiently transfected COS-7 cells (ranging from 48.8 AFU to 141.02 AFU) (Table 2). Basal activity of the wt and mutant FSH receptors was measured (Table 2) and normalized to surface expression as described for the D6.30 mutants (see *D6.30 Mutants*) (Table 2). Like the wt receptor, four mutants (T3.32R, T3.32D, T3.32N, and T3.32S) did not display measurable basal activity (see ratio cAMP/FACS in Table 2). All others mutants displayed varying degree of constitutive activity with T3.32I and T3.32F being the strongest (Table 2). With the exception of T3.32R, all mutants responded to rhFSH stimulation (Fig. 4A). When challenged with rhTSH, six FSHr mutants (T3.32I, T3.32D, T3.32F, T3.32Y, T3.32G, T3.32A) showed increased sensitivity to this promiscuous stimulator. T3.32I and T3.32F were particularly sensitive and caused a dramatic increase of cAMP accumulation in transfected cells upon stimulation by 30 mIU/ml of rhTSH. Three mutants (T3.32R, T3.32N, and T3.32S) behaved like the wt FSHr, with no, or very limited, response to rhTSH (Fig. 4A). In contrast, all mutants, except T3.32R, displayed relaxed sensitivity to rhCG: a definite increase of cAMP accumulation was observed in transfected cells after stimulation by various concentrations of rhCG (30 IU/ml, 100 IU/ml, 300 IU/ml). Similar to the observation for basal activity and sensitivity to rhTSH, in this case also the T3.32I and T3.32F mutants showed the greatest response (Fig. 4B). These results are at variance with the previous report (35) in which no basal activity was detected, nor abnormal sensitivity to TSH for the T3.32I mutant (35).

### T3.32<sup>449</sup>-H7.42<sup>615</sup> Double Mutants

Molecular modeling of the region surrounding T3.32 showed that this residue is located in the cavity

formed by the seven transmembrane helices (Fig. 5A). It is in close proximity with H7.42 (Fig. 5A), a human-specific FSHr residue located one turn above an important network of hydrogen bonds between TM-VI-

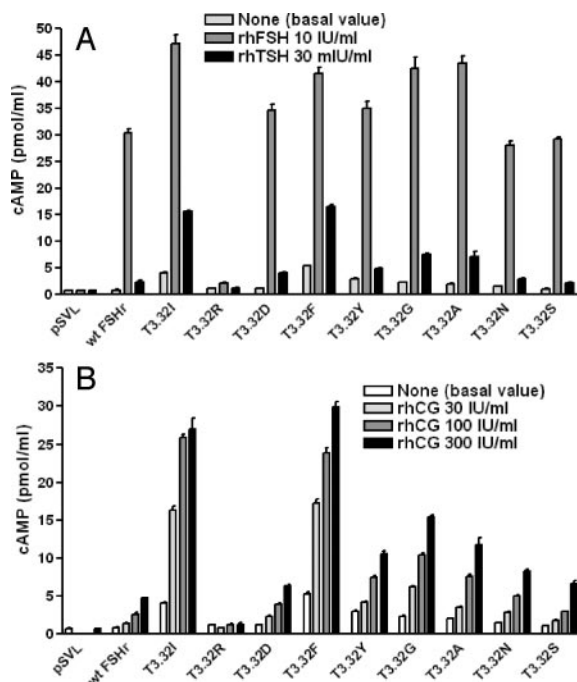


**Fig. 4.** Functional Characterization of T3.32 FSHr Mutants  
A, Levels of cAMP observed with cells transfected with empty pSVL vector, wt hFSHr and T3.32<sup>449</sup> mutants after stimulation with rhFSH (10 IU/ml) and rhTSH (30 mIU/ml) and (B) after stimulation with increasing concentrations of rhCG. COS-7 cells transiently transfected with the various constructs were stimulated by the hormones and intracellular cAMP was determined by RIA. Each graph represents the results of at least two separate experiments. *I* bars represent SE.

**Table 2.** Structure-Function Characteristics of T3.32 Mutants

Construct	FACS (AFU) (Raw Values) <sup>a</sup>		Basal cAMP (pmol/ml) (Raw Values) <sup>a</sup>		cAMP/FACS <sup>b</sup>	Promiscuous Activation
	Mean	Range	Mean	SEM		
pSVL	7.10	±0.61	1.71	0.07		No
wt = T3.32	48.80	±4.12	2.33	0.11	1.48	No
T3.32I	97.69	±4.77	12.48	0.71	11.89	rhCG + rhTSH
T3.32A	124.71	±3.00	5.87	0.18	3.34	rhCG + rhTSH
T3.32F	110.80	±3.06	22.72	0.67	20.26	rhCG + rhTSH
T3.32Y	141.02	±6.59	9.88	0.23	6.10	rhCG + rhTSH
T3.32G	114.42	±6.99	6.75	0.29	4.70	rhCG + rhTSH
T3.32N	69.26	±3.50	3.49	0.11	2.57	rhCG
T3.32R	101.85	±4.54	3.18	0.18	1.55	Total loss of response
T3.32D	55.58	±3.31	2.43	0.39	1.49	rhCG + rhTSH
T3.32S	78.44	±6.33	2.65	0.04	1.32	rhCG

<sup>a</sup> Results from one representative experiment out of a total of two or three experiments.

<sup>b</sup> Basal cAMP was normalized to cell surface expression for each construct, and values were multiplied by 100 for clarity (see *Materials and Methods*).

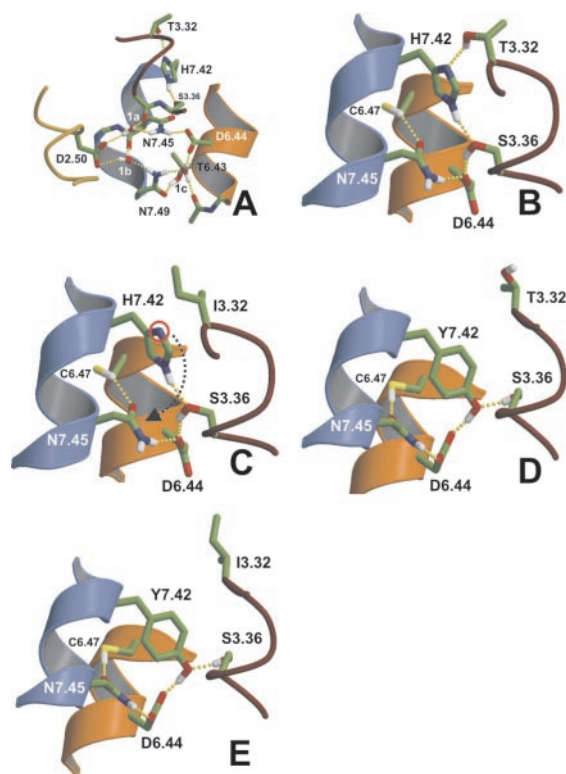


**Fig. 5.** Representative Structures of the Different Models for the 3.32–7.42 Mutant Series

For each of the models, a representative structure was selected from the set collected during the molecular dynamics simulations. A, TM-II-TM-III-TM-VI-TM-VII hydrogen bond network showing the residues D2.50/T3.32/S3.36/D6.44/H7.42/N7.45/N7.49; B, T3.32-H7.42 wt; C, T3.32I (red circle indicates the free N $\delta$  atom of H7.42; black arrow represents the putative movement of H7.42 toward N7.45); D, H7.42Y; and E) T3.32I-H7.42Y double mutant. Helices are represented as *ribbons*, where side chains involved in the investigated interactions are represented as *sticks*. Backbones of transmembrane helices III, VI, and VII are colored in *red*, *orange*, and *blue*, respectively.

TM-VII. This network, involving N7.45, N7.49 and D6.44 has been shown to constrain the TSHr and LH/CGr in the inactive conformation (13, 37, 40). Accordingly, we hypothesized that altering the T3.32/H7.42 region could disturb this TM-VI-TM-VII lock, with consequences on the basal activity of the FSHr.

To explore this possibility, we engineered a series of single and double mutants involving positions 3.32 and 7.42. Single mutants included H7.42Y, H7.42F and H7.42A, in addition to the previously described T3.32I and T3.32F constructs. Double mutants included some combinations of individual single mutants, *i.e.* T3.32I-H7.42Y, T3.32I-H7.42F, T3.32I-H7.42A and T3.32F-H7.42Y (Tables 2 and 3). After transfection in COS-7 cells, expression at the cell surface, basal activity and sensitivity to the various glycoprotein hormones were monitored as described above. Great differences were observed in the level of surface expression, ranging from 23.29 AFU (T3.32F-H7.42A) to 60.24 AFU (T3.32I-H7.42F) (Table 3). Two single mutants of TM-VII (H7.42Y and H7.42F) did not display constitutive activity, whereas H7.42A showed a definite increase in constitutive activity as compared with the essentially silent wt FSHr. When the H7.42Y mutation was engineered on the background of T3.32I (which displays basal activity, see *T3.32 Mutants*), the resulting T3.32I-H7.42Y double mutant was completely silent (Table 3). Similarly the T3.32I-H7.42F double mutant showed lower constitutive activity than T3.32I alone (Tables 2 and 3). On the contrary, when activity is normalized to cell surface expression, the T3.32I-H7.42A double mutant displayed substantial increase of constitutive activation over that of the individual single mutants (see cAMP/FACS ratio in Table 3). Interestingly, combination of the T3.32F mutation (showing definite constitutive activity, Table 3) with H7.42F (essentially devoid of constitutive activity) resulted in a double mutant with even higher constitutive activity (Table 3). As expected, all single and double mutants responded to stimulation by rhFSH (Fig. 6A). When chal-

**Table 3.** Structure-Function Characteristics of H7.42 Single and T3.32-H7.42 Double Mutants

Construct	FACS (AFU) (Raw Values) <sup>a</sup>		Basal cAMP (Raw Values) <sup>a</sup>		cAMP/FACS <sup>b</sup>	Promiscuous Activation
	Mean	Range	Mean	SEM		
pSVL	6.69	±0.81	0.23	0.03		
wt = H7.42	34.88	±4.64	0.41	0.01	0.63	No
T3.32I	55.13	±18.58	1.66	0.09	3.00	rhCG + rhTSH
H7.42Y	60.13	±5.99	0.47	0.03	0.45	No
H7.42F	30.05	±6.39	0.36	0.03	0.56	No
H7.42A	32.80	±8.16	0.92	0.09	2.66	rhCG + rhTSH
T3.32F	46.54	±11.31	2.44	0.04	5.56	rhCG + rhTSH
T3.32I-H7.42Y	56.02	±15.22	0.45	0.03	0.45	No
T3.32I-H7.42F	60.24	±18.95	0.84	0.13	1.14	rhCG + rhTSH
T3.32I-H7.42A	23.29	±9.29	1.28	0.08	6.33	rhCG + rhTSH
T3.32F-H7.42F	51.68	±12.59	3.48	0.13	7.22	rhCG + rhTSH

<sup>a</sup> Results from one representative experiment out of a total on two or three experiments.

<sup>b</sup> Basal cAMP was normalized to cell surface expression for each construct and values were multiplied by 100 for clarity (see *Materials and Methods*).

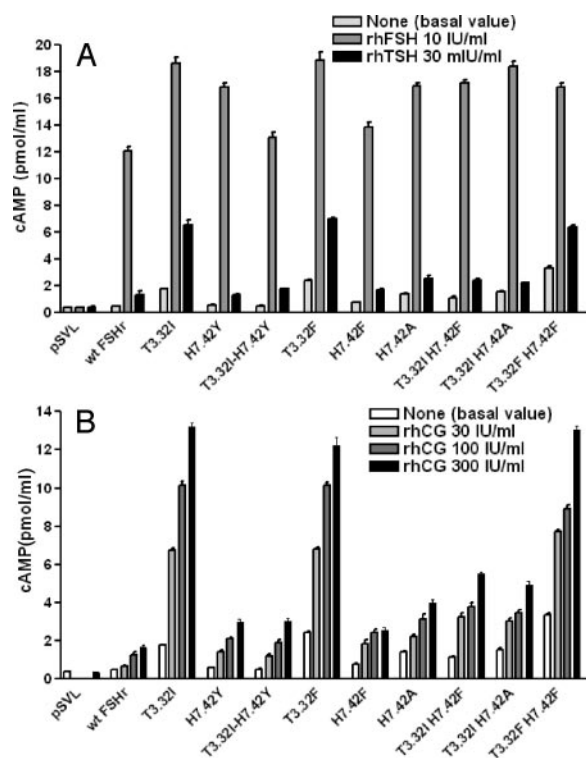


**Fig. 6.** Functional Characterization of T3.32-H7.42 Double Mutants

A, Levels of cAMP observed with cells transfected with empty pSVL vector, wt hFSHr and T3.32<sup>449</sup>-H7.42<sup>615</sup> double mutants after stimulation with rhFSH (10 IU/ml) and rhTSH (30 mIU/ml) and (B) after stimulation with increasing concentrations of rhCG. COS-7 cells transiently transfected with the various constructs were stimulated by the hormones and intracellular cAMP was determined by RIA. Each graph represents the results of at least two separate experiments. / bars represent SE.

lenged with rhTSH, the mutants endowed with the strongest constitutive activity (T3.32I, T3.32F, and T3.32F-H7.42F) displayed a clear increase in sensitivity to rhTSH (Fig. 6A). Similarly, when tested for sensitivity to various concentrations of hCG (30 IU/ml, 100 IU/ml, 300 IU/ml), T3.32I, T3.32F, and T3.32F-H7.42F showed the greatest increase in sensitivity to rhCG (Fig. 6B).

#### Molecular Modeling of the 3.32–7.42 Environment

**The T3.32/H7.42 wt Receptor.** Figure 5A shows a detailed view of the T3.32/S3.36/D6.44/H7.42/N7.45 environment of the molecular model of the hFSHr. These polar side chains, together with the Wat<sub>1</sub> set of water molecules found in the structure of rhodopsin (41) (PDB code: 1L9H), mediate a complex hydrogen bond network. It has been shown that in the hTSHr this network is putatively involved in maintaining the inactive form of the receptor (13). Thus, it seems reasonable to assume that altering the T3.32/H7.42 region could disturb this TM-VI-TM-VII lock leading to changes in interhelical packing and receptor conformation. In wt hFSHr, H7.42

is hydrogen bonding T3.32 and S3.36. N7.45 is interacting with D6.44 and C6.47 (Fig. 5B).

Thus, the imidazole ring of H7.42 is caged in a polar pocket formed by the hydroxyl groups of T3.32 and S3.36 in TM-III and thus locked away from the residues that form the hydrogen bond network between TM-VI and VII (Fig. 5B).

**The T3.32I Mutant.** Substitution of the polar and  $\beta$ -branched T3.32 by the nonpolar and also  $\beta$ -branched Ile induces constitutive activity (Table 2). The lack of any interaction between I3.32 and H7.42 might explain this important phenotype. The hydrogen bond acceptor capability of the N<sub>δ</sub> atom of H7.42 (Fig. 5C, red circle) is not satisfied, making the conformation depicted in Fig. 5C unstable. A reorganization of this network could imply that H7.42 binds the nearest hydrogen bond donor, which is N7.45. Although it is difficult to predict, by molecular dynamics simulations, how interactions between these side chains could evolve toward the constitutively active state, we suggest that the T3.32I mutation would modify the conformation of H7.42, which in turn modifies the conformation of N7.45 (Fig. 5C, black arrow), known to be involved in receptor activation. This hypothesis is supported by the observation that substitutions of T3.32 by a polar amino acid that can interact with H7.42 do not induce constitutive activity: T3.32S, T3.32N, or T3.32D (see Fig. 1 published as supplemental data on The Endocrine Society's Journals Online web site at <http://mend.endojournals.org>). In addition, other aspects, such as bulkiness of the replacing residue at position 3.32, may contribute to the generation of constitutive activity and broadening of specificity (see Discussion).

**H7.42Y and T3.32I/H7.42Y.** Modeling the H7.42Y mutant shows that the introduced tyrosine would hydrogen bond S3.36 and D6.44, without interacting with T3.32 (Fig. 5D). We observe the same interactions of the tyrosine in the model of the double mutant T3.32I/H7.42Y (Fig. 5E). In both of these models and unlike the T3.32I mutant, the equilibrium of the hydrogen bond network between TM-VI and TM-VII is not affected.

#### DISCUSSION

The three paralogous GpHRs display higher sequence identity in their serpentine portion (~70%) than in their ectodomain (~40%). Together with studies involving chimeric and truncated constructs, this led to the conclusion that the ectodomains are responsible for (the specificity of) hormone recognition, whereas the serpentine domains would be interchangeable modules involved in the activation of downstream regulatory cascades. Recent molecular dissection of the leucine-rich repeat motifs implicated in the recognition step by the ectodomains has comforted this view and suggested that natural point mutations of specific residues might lead to promiscuous cross signaling within this gene family (10), as had been shown in a case of gestational thyrotoxicosis (32). Therefore, the identifi-

cation, *in the serpentine portion* of the FSHr, of natural mutations causing its promiscuous activation by hCG, came as a surprise (34–36). One clue was provided by the observation that two of the mutant receptors (D6.30N and T3.32A), in addition to responding abnormally to hCG, displayed substantial constitutive activity and responded also abnormally to high concentrations of TSH (34, 36). When re-explored under the same experimental conditions as the D6.30N, and contrary to the original description (35), the T3.32I mutant displayed also increase in basal activity and abnormal responsiveness to TSH (Ref. 36 and the present study).

Our current model for activation of GpHRs contends that the immediate agonist of the serpentine domain of these receptors would be the activated ectodomain (*i.e.* the ectodomain-hormone complex). The existence of mutations in the ectodomain of all three GpHRs, capable of strongly activating the receptors in the absence of agonist suggested that, contrary to an earlier suggestion (42), there is no need to postulate a direct interaction between the hormone and the serpentine domain of GpHRs to account for activation. In the light of this model, we proposed that lowering of the specificity barrier and increase in constitutive activity, could be linked phenomena: the idea being that a partially unlocked FSHr serpentine would become more easily activated by promiscuous hormone-ectodomain complexes (34).

The present study attempted understanding in molecular terms of the structural and functional consequences of the mutations found in spontaneous OHSS patients. To this aim, the microenvironment of the 3.32 and 6.30 residues of FSHr were probed by site-directed mutagenesis and molecular modeling.

### **An Ionic Lock between Cytoplasmic Ends of TM-III and TM-VI Is Necessary to Constrain the FSHr in the Inactive State and Preserve Its Recognition Specificity**

Activation of rhodopsin-like GPCRs has been suggested to involve a rigid-body motion of TM-III and TM-VI (3, 43). Although the movement of TM-III appeared relatively small, TM-VI underwent a clear counter-clockwise movement (viewed from the extracellular side) directing its cytoplasmic end away from TM-III and toward TM-V (3, 43). Residues of TM-III and TM-VI putatively implicated in stabilizing the resting state have been identified in the LH/CGr (37) and  $\alpha_{1b}$ - and  $\beta_2$ -adrenergic receptors (37–39): they involve the canonical (D/E)R3.50(Y/W) motif (44) at the cytoplasmic border of TM-III and, interestingly, residue 6.30, a partially conserved negatively charged residue of TM-VI (Fig. 3A). The crystal structure of bovine rhodopsin displays a connection between R3.50 and E6.30 (26). According to a currently accepted model, upon receptor activation, the side chain of R3.50 would shift out of a polar pocket (45, 46) formed by E/D3.49 and D/E6.30 (38, 45, 46). An arginine binding

site on the G protein has also been proposed to play a role in this phenomenon (46). In addition, protonation of E/D3.49 has been suggested to weaken the E/D3.49-R3.50 salt bridge upon activation (47, 48), thus facilitating the arginine shift.

Our findings suggest that this cytoplasmic link between TM-III and TM-VI is also present in the inactive hFSHr [and probably other GpHRs as well (37, 49–51)] and plays a critical role in receptor activation. In addition, it provides evidence linking the phenomena of constitutive activity and relaxed specificity. Indeed, a negatively charged residue in position 6.30 is needed to maintain the hFSHr both silent and insensitive to TSH and hCG (Fig. 2, A and B). Interestingly, substitution of D6.30 with Q does not increase basal activity but increases slightly the sensitivity of hFSHr to hCG. Molecular dynamics simulations predict the establishment of two hydrogen bonds between R3.50 and a glutamine in position 6.30 (Fig. 3C) in lieu of the stronger wt ionic interaction. One possible interpretation to this observation is that decrease in functional specificity would be more sensitive than basal activity to (partial) destabilization of the TM-III–TM-VI lock.

Approximately 42% of all rhodopsin-like GPCRs have a negatively charged residue in position 6.30 (52), and the described mechanism could therefore be extended to these receptors. Studies on substitutions of 6.30 in LH/CGr and TSHr, and the phenotype of a deletion mutant in TSHr further support this idea (37, 49–51). However, because a substantial group (32%) of rhodopsin-like GPCRs holds a positively charged residue in this position of TM-VI (52), it is clear that different interactions between the cytoplasmic ends of TM-III and TM-VI must constrain these receptors in the inactive state.

### **T3.32 Is an Important Player in Restraining the FSHr (But Not the TSHr) in the Inactive State**

Residue T3.32 is conserved in the GpHR family, which added to the puzzling observation that its mutation into isoleucine or alanine allowed for promiscuous stimulation of the mutants by hCG and TSH (35, 36). The present study demonstrates, here also, a link between loss of functional specificity and constitutive activity. A polar, preferably not bulky residue is required in position 3.32 to keep the FSHr both silent and normally insensitive to hCG and TSH (Fig. 4, A and B). 3.32 Mutants with bulky nonpolar amino acid substitutions, like 3.32I or 3.32F, show the highest increase in basal cAMP production, accompanied by a strong response to TSH and hCG (Fig. 4, A and B). The importance of a polar group in 3.32 is further demonstrated by the phenotype of the T3.32A mutant, harboring the amino acid substitution found in a patient with spontaneous OHSS (36), and by comparing the functional characteristics of T3.32F and T3.32Y constructs (Table 2). The effect of the bulky nonpolar Phe can be partially suppressed by simply adding a polar group to the aromatic ring. Substitutions of T3.32 with

polar residues (D, N, and S) lead to mutant receptors with basal cAMP levels similar to wt, and the promiscuous response to different hormones is kept to a minimum (Table 2). Surprisingly, the T3.32R mutant has lost completely its responsiveness to all three glycoprotein hormones. We speculate that the large side chain of R3.32 may reach to nearby negative residues, *e.g.* D2.64, which is known to be crucial for receptor activation in the LH/CGr and TSHr (53, 54). A putative interaction between R3.32 and D2.64 would interfere with other D2.64 interactions important for receptor activation in the wt receptor.

Similar to the situation for D6.30, attempts to understand how nonpolar substitutions at position 3.32 cause increase in constitutive activity of the FSHr, prompted us to look for possible interferences with interactions stabilizing the inactive conformation. Molecular modeling showed that T3.32 can hydrogen bond H7.42 (Fig. 5B), which lies close to N7.45, a residue proposed to be important in TM-VI–TM-VII packing in the inactive state (13, 37, 40). Altering the interactions of N7.45 could possibly lead to a disturbance of the TM-VI–TM-VII interaction and induce constitutive receptor activation. Mutation of T3.32 to Ile would make H7.42 free to bind N7.45, hereby disturbing the TM-VI–TM-VII network (Fig. 5C).

We suggest that T3.32 is constraining the FSHr receptor in the inactive state by preventing H7.42 of interacting with N7.45. Of interest, H7.42 is specific to the hFSHr (for sequence alignment, see Fig. 2 published as supplemental data on The Endocrine Society's Journals Online web site at <http://mend.endojournals.org>). All other vertebrate orthologs, including other primates, and GpHR paralogs, harbor a tyrosine in this position. Therefore, it was interesting to explore the phenotype of an H7.42Y mutant, in isolation, or in combination with T3.32 substitutions. In the model of the single H7.42Y mutant, no interaction is possible between T3.32 and Y7.42. Rather, Y7.42 interacts with S3.36 and D6.44 (Fig. 5D). As a consequence, on the Y7.42 background, mutation of T3.32 to Ile has no disturbing effect on the TM-VI–TM-VII interaction (Fig. 5E) and the double mutant displays a wt phenotype. This predicts that nonpolar substitutions of T3.32 are likely to be without effect on the basal activity of non-hFSHr or TSHr (which bear a tyrosine in position 7.42). This is indeed the case for the TSHr (see Fig. 3 in the supplemental data).

When testing experimentally putative interactions in the 3.32–7.42 microenvironment, we discovered that the presence of an aromatic residue in 7.42 (as in all GpHRs except hFSHr) or a histidine plays an important role in stabilizing the inactive state of the receptor. H7.42Y and H7.42F mutants have no basal activity, whereas H7.42A has a basal activity similar to the T3.32I mutant and responds abnormally to hCG. In this respect, comparison of the T3.32I-H7.42Y and T3.32I-H7.42F double mutants is interesting; as already stated, the former displays a wt phenotype, whereas the latter shows some increase in basal activity (Table

3). The T3.32I-H7.42A and T3.32F-H7.42F double mutants are strongly constitutively active, illustrating again the low tolerance of bulky residues in position 3.32.

### Constitutivity and Functional Specificity Are Linked Phenomena in hFSHr: Evolutionary Considerations

Compilation of the data obtained with all FSHr mutants in the present study indicates a relation between constitutive activity and lowering of the specificity barrier for activation by TSH and hCG (see Tables 1–3). Considering that residues 6.30 and 3.32 are conserved in all three GpHRs and that OHSS mutants did not display increase in binding of hCG or TSH (34, 35), this agrees with our earlier suggestion that partial activation of the serpentine portion of the receptor would facilitate the second step of receptor activation by releasing an inhibitory constraint present in the serpentine domain (14, 34, 36). If this model is correct, one would expect other mutations capable of partially releasing the serpentine domain from the inhibitory constraint of the ectodomain to cause similar decrease in functional specificity. This is indeed the case: mutation of serine 273 in the ectodomain of the hFSHr, to isoleucine triggers constitutive activity and causes the mutant to become highly responsive to hCG and TSH (Fig. 7, A and B). Serine 273, or the homologous S281 or S277 residues in the TSHr or LH/CGr, respectively, have been shown to play a key role in the negative constraint exerted by the unliganded ectodomain on the serpentine domain of GpHRs (14, 20, 55–57).

The hFSHr is reportedly more resistant to activation by gain-of-function mutations than the two other GpHRs (28), which suggests that it could be particularly resistant to promiscuous activation. It is tempting to hypothesize that a particularly silent FSHr has been selected, during evolution of higher primates, as a means to cope with the extremely high circulating concentrations of hCG during pregnancy. In line with this view, a previous study has shown that the mouse FSHr displays constitutive activity in the absence of ligand (58). Moreover, another study demonstrated that the rat FSHr is more easily activated by mutations in the serpentine domain than the hFSHr (29). In our hands, the rat FSHr does not display detectable basal activity but, nevertheless, it clearly responds to high dose of hCG (Fig. 7C), in keeping with our suggestion that decrease in functional specificity would be more sensitive than basal activity to (partial) destabilization of the serpentine domain (see above).

The relation between basal activity and functional specificity is a characteristic of the FSHr, which is not shared by the other GpHRs. All T3.32, D6.30, and homologs of S273 single mutants have been engineered and tested in the TSHr background. Whereas increase in constitutive activity was readily detected in the D6.30 and S281 mutants [as already observed

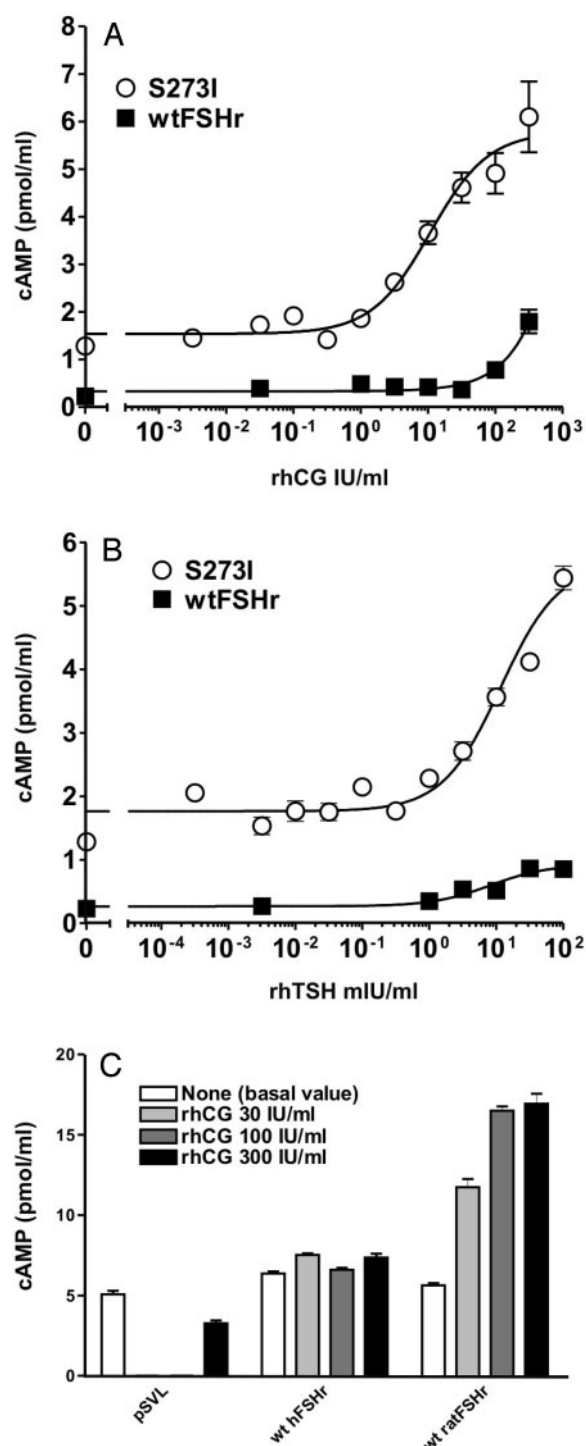


**Fig. 7.** Functional Characterization of an S273I FSHr Mutant and of wt rat FSHr

A, Concentration-action curve for wt hFSHr and S273I under stimulation by increasing concentration of rhCG. COS-7 cells transiently transfected with the various constructs were stimulated by increasing concentrations of rhCG and intracellular cAMP was determined by RIA. B, Concentration-action curve for wt hFSHr and S273I under stimulation by increasing concentration of rhTSH. The Prism computer program (GraphPad Software, Inc.) was used for curve fitting and for EC<sub>50</sub> calculation. Each curve is representative of at

previously (34, 55–57)], no decrease in specificity could be observed. This leads to the interesting suggestion that different pathways have been followed during primate evolution to avoid promiscuous stimulation of the TSHr and FSHr by hCG. In the former, specificity is solely built in the LRR portion of the ectodomain of the receptor (10, 32, 33), whereas in the latter, it would be exerted both by the ectodomain and the serpentine portion.

## MATERIALS AND METHODS

### Numbering Scheme of GPCRs

The standardized numbering scheme of Ballesteros and Weinstein, which allows the identification of residues in the transmembrane segments of different receptors, was used throughout the manuscript (59).

### Reagents

Plasmid pBluescript SK<sup>+</sup> was obtained from Stratagene (La Jolla, CA); plasmid pSVL was obtained from Amersham Pharmacia Biotech (Roosendaal, The Netherlands). Restriction enzymes were obtained from Life Technologies, Inc. (Merelbeke, Belgium) and New England Biolabs (Beverly, MA). *Pfu* Turbo polymerase was obtained from Stratagene. Monoclonal antibody 5B2 was obtained by genetic immunization (60) with the cDNA encoding the hFSHr. rhCG was from Sigma (St. Louis, MO), rhFSH from Organon Belge (Brussels, Belgium) and rhTSH from Genzyme Corp. (Cambridge, MA).

### Construction of the FSHr Mutants

Mutations were introduced in the hFSHr by site mutagenesis as described previously (14). The sequences of the primers are available upon request. The natural *Xba*I site in position 665 of hFSHr cDNA was eliminated to allow its cloning in pSVL between *Xho*I and *Xba*I sites. The appropriate mutated portions of SK<sup>+</sup> hFSHr mutants were subcloned in the pSVL-hFSHr cDNA using natural restriction sites. The strategy of construction of each mutant is available upon request. All constructs were amplified in DH5 $\alpha$ F' competent cells, and recombinant DNA from selected clones was purified and sequenced for confirmation of the nucleotide sequences of the PCR-generated areas.

### Transfection Experiments

COS-7 cells were used for all transient expression experiments, which were performed according two protocols. The first standard protocol (14) was used for accurate determination of constitutive activity. Briefly, 300,000 cells were seeded in 3.5 culture dishes at d 1, and transfected at d 2 by diethylaminoethyl-

least two separate experiments. C, Levels of cAMP observed with cells transfected with empty pSVL vector, wt hFSHr, and wt rat FSHr after stimulation with increasing concentrations of rhCG. COS-7 cells transiently transfected with the various constructs were stimulated by increasing concentrations of rhCG and intracellular cAMP was determined by RIA. Each graph represents the results of at least two separate experiments. *I bars* represent SE.

dextran method, as described previously (14). Two days after transfection, cells were used for cAMP determinations and flow immunocytofluorometry. The second 24-well protocol was used for all experiments exploring sensitivity to hormones, with the aim of minimizing the amount of hormones needed. Briefly, 2 million cells were seeded in 10-cm dishes at d 1 and transfected at d 2 as described above. At d 3, cells were trypsinized, detached and centrifuged at  $700 \times g$  for 2 min. They were suspended in 16 ml of culture medium and seeded (1 ml/well) in 24-well plates (Nunc Brand Products, Sanbio b.v., Uden, The Netherlands). At d 5, cells were used for cAMP determinations and flow immunocytofluorometry. Duplicate dishes were used for each assay. Each experiment was repeated at least twice. Cells transfected with pSVL alone were always run as controls.

#### Quantification of Cell Surface Expression of FSHr Constructs by FACS

Cells were prepared as previously described (60). After detachment, they were centrifuged at  $500 \times g$  at 4°C for 3 min and the supernatant was removed by inversion. They were incubated for 30 min at room temperature with 100  $\mu$ l PBS-BSA 0.1% containing the 5B2 monoclonal antibody. Cells were then washed with 4 ml PBS-BSA 0.1% and centrifuged as above. They were incubated on ice in the dark with fluorescein-conjugated  $\mu$ -chain-specific goat antimouse IgG (Sigma) in the same buffer. Propidium iodide (10  $\mu$ g/ml) was used for detection of damaged cells that were excluded from the analysis. Cells were washed and resuspended in 300  $\mu$ l PBS-BSA 0.1%. The fluorescence of 10,000 cells/tube was assayed by a FACScan flow cytometer (Becton Dickinson and Co., Erembodegem, Belgium). Cells transfected by pSVL alone and by pSVL-FSHr wt cDNA were always run as negative and positive controls, respectively.

#### Determination of cAMP Production

For cAMP determination, culture medium was removed 48 h after transfection and replaced by Krebs-Ringer-HEPES buffer for 30 min. Thereafter, cells were incubated for 60 min in fresh Krebs-Ringer-HEPES buffer supplemented with 25  $\mu$ M of the phosphodiesterase inhibitor Rolipram (Laboratoire Logeais, Paris, France) and graded concentrations of the various hormones (rhCG, rhFSH, and rhTSH). After 1 h incubation, the medium was discarded and replaced with HCl 0.1 M. The cell extracts were dried under vacuum, resuspended in water, and diluted appropriately for cAMP measurements according to the method of Brooker *et al.* (61). cAMP concentrations were determined in quadruplicate on extracts from duplicate transfection dishes or wells. Results are expressed in picomoles per milliliter.

#### Normalization of cAMP Values to Surface Expression of Mutants

Basal cAMP was normalized to cell surface expression for each construct by calculating the ratio of cAMP/FACS values. Receptor-dependent cAMP accumulation (cAMP in receptor-transfected cells – cAMP in pSVL-transfected cells) was divided by the receptor-dependent fluorescence measured by flow immunocytofluorometry (fluorescence of receptor-transfected cells – fluorescence of the pSVL-transfected cells).

Concentration-action curves were fitted with Prism version 3.03 (GraphPad Software, Inc., San Diego, CA).

#### Conversion between IU/ml and ng/ml

A quantity of 1 IU/ml of rhCG corresponds to 62 ng/ml, or 2 nM (Sigma); 1 IU/ml of rhFSH corresponds to 100 ng/ml, or 3.3 nM (Puregon, Organon); and 1 mIU/ml of rhTSH equals 125 ng/ml, or 4 nM (Thyrogen, Genzyme).

#### Molecular Modeling and Molecular Dynamics Simulation of the Transmembrane Bundle

A model of the transmembrane domain of the FSHr plus helix 8 that expands parallel to the membrane was constructed by homology modeling using the crystal structure of bovine rhodopsin (PDB code 1L9H) (26) as template. The residues considered to be most conserved in the Class A family of GPCRs were aligned in both sequences. These include N<sup>55</sup>-N1.50<sup>360</sup> (the superscripts represent the residue numbering in the rhodopsin structure and hFSHr sequence, respectively, and 1.50 is the standardized nomenclature (59), L<sup>79</sup>-L2.46<sup>404</sup>, R<sup>135</sup>-R3.50<sup>467</sup>, W<sup>161</sup>-W4.50<sup>494</sup>, Y<sup>223</sup>-Y5.58<sup>549</sup>, P<sup>267</sup>-P6.50<sup>587</sup>, P<sup>303</sup>-P7.50<sup>623</sup>. The molecular models for the mutant receptors were built from the derived model of wt FSHr, by changing the atoms implicated in the amino acid substitutions by interactive computer graphics. These structures were placed in a cubic box of 83 Å × 67 Å × 65 Å containing a palmitoyloleoylphosphatidylcholine lipid bilayer, constructed from the model available at <http://www.ks.uiuc.edu/~ilya/Membranes/> by adding both lipids and water molecules. The final box of the different models contain approximately 88 palmitoyloleoylphosphatidylcholine, approximately 9580 waters, and 228 protein residues including the blocking helix caps (~44000 atoms).

The atoms of the lipid and water molecules were first energy minimized (500 steps), followed by a minimization (500 steps) of the whole system. Hereafter, full unrestrained molecular dynamics was initiated, starting with a heating (from –273 to 27°C in 15 psec), equilibration (until 100 psec) and a production (100–200 psec) run at constant pressure using the particle Mesh Ewald method to evaluate electrostatic interactions. Structures were collected every 10 psec for analysis purposes during the production run. Atom-atom distances were calculated with the Carnal program of Amber 7 (62). The molecular dynamics simulations were carried out with the Sander module of Amber 7 (62, 62a), the all-atom force field (63), SHAKE bond constraints in all bonds, a 2-fsec integration time step, and constant temperature of 27°C coupled to a heat bath. Unrestrained molecular dynamics simulation of the wt FSHr was performed for 500 psec and a plot of all-atom root mean square deviation (rmsd) vs. time was drawn for the protein portion of the system relative to the initial model (see above). The motions of the transmembrane helices and side chains were found to occur during the first 100 psec of simulation, as shown by the significant change in rmsd. Thereafter, the structures collected during the following 100- to 200-psec period were shown to be representative of longer simulation times (data not shown).

#### Acknowledgments

We thank Xavier Deupí for assistance in the molecular dynamics simulations.

Received January 29, 2004. Accepted May 18, 2004.

Address all correspondence and requests for reprints to: Dr. Sabine Costagliola, IRIBHM, Université Libre de Bruxelles, Campus Erasme, Route de Lennik 808, B-1070 Brussels. E-mail: scostag@ulb.ac.be.

This work was supported by the Belgian State, Prime Minister's office, Service for Sciences, Technology and Culture; the Interuniversity Attraction Poles of the Belgian Federal Office for Scientific, Technical and Cultural Affairs; grants from the Fonds de la Recherche Scientifique, Fonds National de la Recherche Scientifique (FNRS), Association Recherche Biomédicale et Diagnostique, and BRAHMS Diagnostics; the European Community (LSHB-CT-2003-503337); and Comision Interministerial de Ciencia Tecnologia (SAF2002-01509). Computer facilities were provided by the Centre de Computació i Comunicacions de

Catalunya. S.C. is Research Associate at the FNRS. P.R. was supported by a grant from Institut National de la Santé et de la Recherche Médicale, AVENIR 2001.

L.M. and J.J.J.V.D. contributed equally to this work.

## REFERENCES

- Ascoli M, Fanelli F, Segaloff DL 2002 The lutropin/choriogonadotropin receptor, a 2002 perspective. *Endocr Rev* 23:141–174
- Dias JA, Cohen BD, Lindau-Shepard B, Nechamen CA, Peterson AJ, Schmidt A 2002 Molecular, structural, and cellular biology of follitropin and follitropin receptor. *Vitam Horm* 64:249–322
- Gether U 2000 Uncovering molecular mechanisms involved in activation of G protein-coupled receptors. *Endocr Rev* 21:90–113
- Szkudlinski MW, Fremont V, Ronin C, Weintraub BD 2002 Thyroid-stimulating hormone and thyroid-stimulating hormone receptor structure-function relationships. *Physiol Rev* 82:473–502
- Hsu SY, Liang SG, Hsueh AJW 1998 Characterization of two LGR genes homologous to gonadotropin and thyrotropin receptors with extracellular leucine-rich repeats and a G protein-coupled, seven-transmembrane region. *Mol Endocrinol* 12:1830–1845
- Braun T, Schofield PR, Sprengel R 1991 Amino-terminal leucine-rich repeats in gonadotropin receptors determine hormone selectivity. *EMBO J* 10:1885–1890
- Cornelis S, Uttenweiler-Joseph S, Panneels V, Vassart G, Costagliola S 2001 Purification and characterization of a soluble bioactive amino-terminal extracellular domain of the human thyrotropin receptor. *Biochemistry* 40:9860–9869
- Remy JJ, Nespoulous C, Grosclaude J, Grebert D, Couture L, Pajot E, Salesse R 2001 Purification and structural analysis of a soluble human choriongonadotropin hormone-receptor complex. *J Biol Chem* 276:1681–1687
- Schmidt A, MacColl R, Lindau-Shepard B, Buckler DR, Dias JA 2001 Hormone-induced conformational change of the purified soluble hormone binding domain of follitropin receptor complexed with single chain follitropin. *J Biol Chem* 276:23373–23381
- Smits G, Campillo M, Govaerts C, Janssens V, Richter C, Vassart G, Pardo L, Costagliola S 2003 Glycoprotein hormone receptors: determinants in leucine-rich repeats responsible for ligand specificity. *EMBO J* 22:2692–2703
- Vischer HF, Granneman JCM, Bogerd J 2003 Opposite contribution of two ligand-selective determinants in the N-terminal hormone-binding exodomain of human gonadotropin receptors. *Mol Endocrinol* 17:1972–1981
- Kajava AV, Kobe B 2002 Assessment of the ability to model proteins with leucine-rich repeats in light of the latest structural information. *Protein Sci* 11:1082–1090
- Govaerts C, Lefort A, Costagliola S, Wodak SJ, Ballesteros JA, Van Sande J, Pardo L, Vassart G 2001 A conserved Asn in transmembrane helix 7 is an on/off switch in the activation of the thyrotropin receptor. *J Biol Chem* 276:22991–22999
- Vlaeminck-Guillem V, Ho SC, Rodien P, Vassart G, Costagliola S 2002 Activation of the cAMP pathway by the TSH receptor involves switching of the ectodomain from a tethered inverse agonist to an agonist. *Mol Endocrinol* 16:736–746
- Kobilka BK 2002 Agonist-induced conformational changes in the  $\beta(2)$  adrenergic receptor. *J Pept Res* 60:317–321
- Vassart G, Pardo L, Costagliola S 2004 A molecular dissection of the glycoprotein hormone receptors. *Trends Biochem Sci* 29:119–126
- Samama P, Cotecchia S, Costa T, Lefkowitz RJ 1993 A mutation-induced activated state of the  $\beta(2)$ -adrenergic receptor—extending the ternary complex model. *J Biol Chem* 268:4625–4636
- Meng EC, Bourne HR 2001 Receptor activation: what does the rhodopsin structure tell us? *Trends Pharmacol Sci* 22:587–593
- Gether U, Asmar F, Meinhild AK, Rasmussen SG 2002 Structural basis for activation of G-protein-coupled receptors. *Pharmacol Toxicol* 91:304–312
- Parma J, Duprez L, VanSande J, Hermans J, Rocmans P, VanVliet G, Costagliola S, Rodien P, Dumont JE, Vassart G 1997 Diversity and prevalence of somatic mutations in the thyrotropin receptor and G(s) $\alpha$  genes as a cause of toxic thyroid adenomas. *J Clin Endocrinol Metab* 82:2695–2701
- Shenker A 2002 Activating mutations of the lutropin choriongonadotropin receptor in precocious puberty. *Receptors Channels* 8:3–18
- Duprez L, Parma J, VanSande J, Allgeier A, Leclere J, Schwart C, Delisle MJ, Decoulx M, Orgiazzi J, Dumont J, Vassart G 1994 Germline mutations in the thyrotropin receptor gene cause non-autoimmune autosomal-dominant hyperthyroidism. *Nat Genet* 7:396–401
- Kopp P, VanSande J, Parma J, Duprez L, Gerber H, Joss E, Jameson JL, Dumont JE, Vassart G 1995 Brief report—congenital hyperthyroidism caused by a mutation in the thyrotropin-receptor gene. *N Engl J Med* 332:150–154
- Tonacchera M, VanSande J, Cetani F, Swillens S, Schwart C, Winiszewski P, Portmann L, Dumont JE, Vassart G, Parma J 1996 Functional characteristics of three new germline mutations of the thyrotropin receptor gene causing autosomal dominant toxic thyroid hyperplasia. *J Clin Endocrinol Metab* 81:547–554
- Themmen APN, Huhtaniemi IT 2000 Mutations of gonadotropins and gonadotropin receptors: elucidating the physiology and pathophysiology of pituitary-gonadal function. *Endocr Rev* 21:551–583
- Palczewski K, Kumasaka T, Hori T, Behnke CA, Motoshima H, Fox BA, Le Trong I, Teller DC, Okada T, Stenkamp RE, Yamamoto M, Miyano M 2000 Crystal structure of rhodopsin: a G protein-coupled receptor. *Science* 289:739–745
- Clayson S, Govaerts C, Lefort A, Van Sande J, Costagliola S, Pardo L, Vassart G 2002 A conserved Asn in TM7 of the thyrotropin receptor is a common requirement for activation by both mutations and its natural agonist. *FEBS Lett* 517:195–200
- Kudo M, Osuga Y, Kobilka BK, Hsueh AJW 1996 Transmembrane regions V and VI of the human luteinizing hormone receptor are required for constitutive activation by a mutation in the third intracellular loop. *J Biol Chem* 271:22470–22478
- Tao YX, Mizrahi D, Segaloff DL 2002 Chimeras of the rat and human FSH receptors (FSHRs) identify residues that permit or suppress transmembrane 6 mutation-induced constitutive activation of the FSHR via rearrangements of hydrophobic interactions between helices 6 and 7. *Mol Endocrinol* 16:1881–1892
- Gromoll J, Simoni M, Nieschlag E 1996 An activating mutation of the follicle-stimulating hormone receptor autonomously sustains spermatogenesis in a hypophysectomized man. *J Clin Endocrinol Metab* 81:1367–1370
- Glinoer D 1997 The regulation of thyroid function in pregnancy: pathways of endocrine adaptation from physiology to pathology. *Endocr Rev* 18:404–433
- Rodien P, Bremont C, Parma J, Van Sande J, Costagliola S, Luton JP, Vassart G, Duprez L 1998 Familial gestational hyperthyroidism caused by a mutant thyrotropin receptor hypersensitive to human chorionic gonadotropin. *N Engl J Med* 339:1823–1826
- Smits G, Govaerts C, Nubourgh I, Pardo L, Vassart G, Costagliola S 2002 Lysine 183 and glutamic acid 157 of

- the TSH receptor: two interacting residues with a key role in determining specificity toward TSH and human CG. *Mol Endocrinol* 16:722–735
34. Smits G, Olatunbosun O, Delbaere A, Pierson R, Vassart G, Costagliola S 2003 Ovarian hyperstimulation syndrome due to a mutation in the follicle-stimulating hormone receptor. *N Engl J Med* 349:760–766
  35. Vasseur C, Rodien P, Beau I, Desroches A, Gerard C, de Poncheville L, Chaplot S, Savagner F, Croue A, Mathieu E, Lahlou N, Descamps P, Misrahi M 2003 A chorionic gonadotropin-sensitive mutation in the follicle-stimulating hormone receptor as a cause of familial gestational spontaneous ovarian hyperstimulation syndrome. *N Engl J Med* 349:753–759
  36. Montanelli L, Delbaere A, Di Carlo C, Nappi C, Smits G, Vassart G, Costagliola S 2004 A mutation in the follicle-stimulating hormone receptor as a cause of familial spontaneous ovarian hyperstimulation syndrome. *J Clin Endocrinol Metab* 89:1255–1258
  37. Angelova K, Fanelli F, Puett D 2002 A model for constitutive lutropin receptor activation based on molecular simulation and engineered mutations in transmembrane helices 6 and 7. *J Biol Chem* 277:32202–32213
  38. Ballesteros JA, Jensen AD, Liapakis G, Rasmussen SGF, Shi L, Gether U, Javitch JA 2001 Activation of the  $\beta(2)$ -adrenergic receptor involves disruption of an ionic lock between the cytoplasmic ends of transmembrane segments 3 and 6. *J Biol Chem* 276:29171–29177
  39. Greasley PJ, Fanelli F, Rossier O, Abuin L, Cotecchia S 2002 Mutagenesis and modelling of the  $\alpha(1b)$ -adrenergic receptor highlight the role of the helix 3/helix 6 interface in receptor activation. *Mol Pharmacol* 61:1025–1032
  40. Angelova K, Narayan P, Simon JP, Puett D 2000 Functional role of transmembrane helix 7 in the activation of the heptahelical lutropin receptor. *Mol Endocrinol* 14:459–471
  41. Okada T, Fujiyoshi Y, Silow M, Navarro J, Landau EM, Shichida Y 2002 Functional role of internal water molecules in rhodopsin revealed by x-ray crystallography. *Proc Natl Acad Sci USA* 99:5982–5987
  42. Ji I, Ji TH 1991 Human choriogonadotropin binds to a lutropin receptor with essentially no N-terminal extension and stimulates camp synthesis. *J Biol Chem* 266:13076–13079
  43. Farrens DL, Altenbach C, Yang K, Hubbell WL, Khorana HG 1996 Requirement of rigid-body motion of transmembrane helices for light activation of rhodopsin. *Science* 274:768–770
  44. Oliveira L, Paiva ACM, Vriend G 1993 A common motif in G-protein-coupled 7 transmembrane helix receptors. *J Comput Aided Mol Des* 7:649–658
  45. Scheer A, Fanelli F, Costa T, DeBenedetti PG, Cotecchia S 1996 Constitutively active mutants of the  $\alpha(1B)$ -adrenergic receptor: role of highly conserved polar amino acids in receptor activation. *EMBO J* 15:3566–3578
  46. Oliveira L, Paiva ACM, Vriend G 1999 A low resolution model for the interaction of G proteins with G protein-coupled receptors. *Protein Eng* 12:1087–1095
  47. Ghanouni P, Schambye H, Seifert R, Lee TW, Rasmussen SGF, Gether U, Kobilka BK 2000 The effect of pH on  $\beta(2)$  adrenoceptor function—evidence for protonation-dependent activation. *J Biol Chem* 275:3121–3127
  48. Arnis S, Fahmy K, Hofmann KP, Sakmar TP 1994 A conserved carboxylic-acid group mediates light-dependent proton uptake and signaling by rhodopsin. *J Biol Chem* 269:23879–23881
  49. Parma J, Duprez L, VanSande J, Cochaux P, Gervy C, Mockel J, Dumont J, Vassart G 1993 Somatic mutations in the thyrotropin receptor gene cause hyperfunctioning thyroid adenomas. *Nature* 365:649–651
  50. Kosugi S, Mori T, Shenker A 1998 An anionic residue at position 564 is important for maintaining the inactive conformation of the human lutropin/choriogonadotropin receptor. *Mol Pharmacol* 53:894–901
  51. Wonerow P, Schoneberg T, Schultz G, Gudermann T, Paschke R 1998 Deletions in the third intracellular loop of the thyrotropin receptor—a new mechanism for constitutive activation. *J Biol Chem* 273:7900–7905
  52. Horn F, Bettler E, Oliveira L, Campagne F, Cohen FE, Vriend G 2003 GPCRDB information system for G protein-coupled receptors. *Nucleic Acids Res* 31:294–297
  53. Ji I, Ji TH 1993 Receptor activation is distinct from hormone-binding in intact lutropin-choriogonadotropin receptors and Asp (397) is important for receptor activation. *J Biol Chem* 268:20851–20854
  54. Kosugi S, Matsuda A, Hai N, Aoki N, Sugawa H, Mori T 1997 Aspartate-474 in the first exoplasmic loop of the thyrotropin receptor is crucial for receptor activation. *FEBS Lett* 406:139–141
  55. Nakabayashi K, Kudo M, Kobilka B, Hsueh AWJ 2000 Activation of the luteinizing hormone receptor following substitution of Ser-277 with selective hydrophobic residues in the ectodomain hinge region. *J Biol Chem* 275:30264–30271
  56. Ho SC, Van Sande J, Lefort A, Vassart G, Costagliola S 2001 Effects of mutations involving the highly conserved S281HCC motif in the extracellular domain of the thyrotropin (TSH) receptor on TSH binding and constitutive activity. *Endocrinology* 142:2760–2767
  57. Kopp P, Jameson JL, Roe TF 1997 Congenital nonautoimmune hyperthyroidism in a nonidentical twin caused by a sporadic germline mutation in the thyrotropin receptor gene. *Thyroid* 7:765–770
  58. Baker PJ, Pakarinen P, Huhtaniemi IT, Abel MH, Charlton HM, Kumar TR, O’Shaughnessy PJ 2003 Failure of normal Leydig cell development in follicle-stimulating hormone (FSH) receptor-deficient mice, but not FSH  $\beta$ -deficient mice: role for constitutive FSH receptor activity. *Endocrinology* 144:138–145
  59. Ballesteros JA, Weinstein H 1995 Integrated methods for modelling G-protein-coupled receptors. *Methods Neurosci* 366–428
  60. Costagliola S, Khoo D, Vassart G 1998 Production of bioactive amino-terminal domain of the thyrotropin receptor via insertion in the plasma membrane by a glycosylphosphatidylinositol anchor. *FEBS Lett* 436:427–433
  61. Brooker G, Harper JF, Terasaki WL, Moylan RD 1979 Radioimmunoassay of cyclic AMP and cyclic GMP. *Adv Cyclic Nucleotide Res* 10:1–33
  62. Case DA, Pearlman DA, Caldwell JW, Cheatham III TE, Wang J, Ross WS, Simmerling CL, Darden TA, Merz KM, Stanton RV, Cheng AL, Vincent JJ, Crowley M, Tsui V, Gohlke H, Radmer RJ, Duan Y, Pitara J, Massova I, Seibel GL, Singh UC, Weiner PK, Kollman PA 2002 AMBER 7. University of California, San Francisco
  - 62a. Pearlman DA, Case DA, Caldwell JW, Ross WS, Cheatham TE, DeBolt S, Ferguson DM, Seibel GL, Kollman PA 1995 AMBER, a package of computer programs for applying molecular mechanics, normal mode analysis, molecular dynamics and free energy calculations to simulate the structural and energetic properties of molecules. *Comput Phys Commun* 91:1–41
  63. Cornell WD, Cieplak P, Bayly CI, Gould IR, Merz KM, Ferguson DM, Spellmeyer DC, Fox T, Caldwell JW, Kollman PA 1995 A 2nd generation force-field for the simulation of proteins, nucleic-acids, and organic-molecules. *J Am Chem Soc* 117:5179–5197